ORGANIC LETTERS

2008
Vol. 10, No. 24
5545−5548

9,10,19,20-Tetraarylporphycenes

K. S. Anju,[†] S. Ramakrishnan,[†] Ajesh P. Thomas,[†] Eringathodi Suresh,[‡] and Alagar Srinivasan*,[†]

Photosciences and Photonics Section, Chemical Sciences and Technology Division, National Institute for Interdisciplinary Science and Technology (NIIST-CSIR), Trivandrum-695019, Kerala, India, and Analytical Science Discipline, Central Salt and Marine Chemical Research Institute (CSMCRI-CSIR), Bhavnagar-364002, Gujarat, India

indiansrini@gmail.com

Received October 10, 2008

ABSTRACT

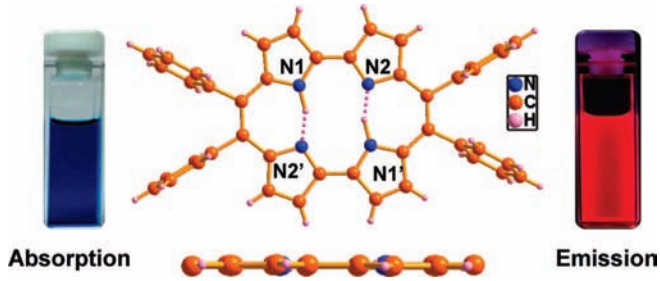

***meso*-Tetraarylporphycenes, structural isomers of *meso*-tetraarylporphyrins, were synthesized by the acid-catalyzed oxidative coupling reaction for the first time which is an alternative synthetic methodology to the traditional McMurry coupling reaction. The structure of the macrocycle and Ni(II) complex are characterized by single-crystal X-ray diffraction analyses where both form 1-D supramolecular assembly.**

Porphycene (**2**, **3**), an isomer of porphyrin (**1**) with $C_{20}H_{14}N_4$ in its macrocyclic core, is a potential candidate in the area of photodynamic therapy (PDT) due to immense absorption in the far red region of the visible spectrum.[1] It was first reported by Vogel and co-workers as a planar, aromatic macrocycle formally known as [18]porphyrin-(2.0.2.0).[2a] Since then, a series of porphycene derivatives[1,2] such as tetraalkyl[2b]/tetraaryl (**2a**)[2f−h] /octaalkyl (**2b**)[2d,e] and their metal complexes[3] have been reported. The substituents are confined to the β-position of the pyrrole rings, and these compounds are considered as isomers of octaethylporphyrin (OEP, **1a**). In addition, *meso*-tetraalkylporphycenes (**3**) were also synthesized by Vogel et al.[2c] All of the derivatives were

[†] National Institute for Interdisciplinary Science and Technology.
[‡] Central Salt and Marine Chemical Research Institute.

(1) (a) Sanchez-Garcia, D.; Sessler, J. L. *Chem. Soc. Rev.* **2008**, *37*, 215–232. (b) Stockert, J. C.; Canete, M.; Juarranz, A.; Villanueva, A.; Horoin, R. W.; Borrell, J. I.; Teixido, J.; Nonell, S. *Curr. Med. Chem.* **2007**, *14*, 997–1026.

(2) (a) Vogel, E.; Kocher, M.; Schmickler, H.; Lex, J. *Angew. Chem., Int. Ed. Engl.* **1986**, *25*, 257–259. (b) Vogel, E.; Balci, M.; Pramod, K.; Koch, P.; Lex, J.; Ermer, O. *Angew. Chem., Int. Ed. Engl.* **1987**, *26*, 928–931. (c) Vogel, E.; Kocher, M.; Lex, J.; Ermer, O. *Isr. J. Chem.* **1989**, *29*, 257–266. (d) Vogel, E.; Koch, P.; Hou, X.-L.; Lex, J.; Lausmann, M.; Kisters, M.; Aukauloo, M. A.; Richard, P.; Guilard, R. *Angew. Chem., Int. Ed. Engl.* **1993**, *32*, 1600–1604. (e) Guilard, R.; Aukauloo, M. A.; Tardieux, C.; Vogel, E. *Synthesis* **1995**, 1480–1482. (f) Nonell, S.; Bou, N.; Borrell, J. I.; Teixido, J.; Villanueva, A.; Juarranz, A.; Canete, M. *Tetrahedron Lett.* **1995**, *36*, 3405–3408. (g) Gavalda, A.; Borrell, J. I.; Teixido, J.; Nonell, S.; Arad, O.; Grau, R.; Canete, M.; Juarranz, A.; Villanuea, A.; Stockert, J. C. *J. Porphyrins Phthalocyanines* **2001**, *5*, 846–852. (h) Arad, O.; Morros, J.; Batllori, X.; Teixido, J.; Nonell, S.; Borrell, J. I. *Org. Lett.* **2006**, *8*, 847–850.

(3) (a) Gisselbrecht, J. P.; Gross, M.; Kocher, M.; Lausmann, M.; Vogel, E. *J. Am. Chem. Soc.* **1990**, *112*, 8618–8620. (b) Oertling, W. A.; Wu, W.; Lopez-Garriga, J. J.; Kim, Y.; Chang, C. K. *J. Am. Chem. Soc.* **1991**, *113*, 127–134. (c) Li, Z.-Y.; Huang, J.-S.; Che, C.-M.; Chang, C. K. *Inorg. Chem.* **1992**, *31*, 2670–2672. (d) Kadish, K. M.; Van Caemebecke, E.; Boulas, P.; D'Souza, F.; Vogel, E.; Kisters, M.; Medforth, C. J.; Smith, K. M. *Inorg. Chem.* **1993**, *32*, 4177–4178. (e) Lausmann, M.; Zimmer, I.; Lex, J.; Lueken, H.; Wieghardt, K.; Vogel, E. *Angew. Chem., Int. Ed. Engl.* **1994**, *33*, 736–739. (f) D'Souza, F.; Boulas, P.; Aukauloo, A. M.; Guilard, R.; Kisters, M.; Vogel, E.; Kadish, K. M. *J. Phys. Chem.* **1994**, *98*, 11885–11891. (g) Canete, M.; Ortiz, A.; Juarranz, A.; Villanueva, A.; Nonell, S.; Borrell, J. I.; Teixido, J.; Stockert, J. C. *Anti-Cancer Drug Des.* **2000**, *15*, 143. (h) Flower, C. J.; Sessler, J. L.; Lynch, V.; Waluk, J.; Gebauer, A.; Lex, J.; Heger, A.; Zuniga-y-Rivero, F.; Vogel, E. *Chem.—Eur. J.* **2002**, *8*, 3485–3496.

10.1021/ol802351r CCC: $40.75
Published on Web 11/17/2008

synthesized through McMurry coupling reactions, which is the only known methodology available to date.[1,2] However, to the best of our knowledge, *meso*-tetraarylporphycene, the structural isomer of *meso*-tetraarylporphyrin (TPP, **1b**), is not known. Herein, we wish to report the synthesis, structural characterization and coordination studies of *meso*-tetraarylporphycene. Instead of the traditional McMurry coupling reactions, we adopted acid-catalyzed oxidative couplings[4] for the synthesis of *meso*-tetraaryl derivatives and the structural features favor the formation of divalent metal complexes.

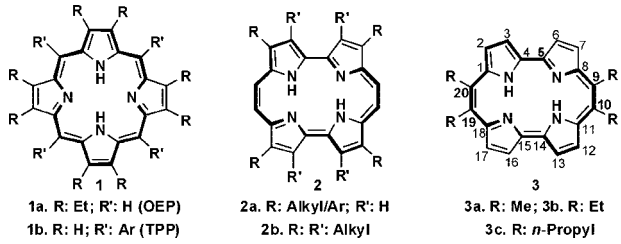

The synthesis of the target macrocycle and its metal complexes is depicted in Scheme 1, where the synthesis

Scheme 1. Syntheses of **6**−**9**

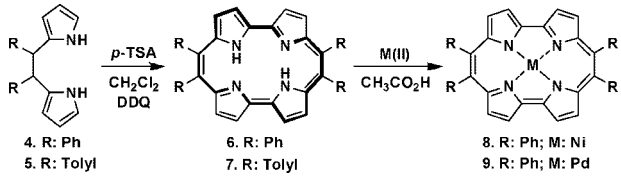

involved three steps. The initial step is the quantitative conversion of benzoin and/or benzil to 1,2-diphenylethane-1,2-diol by using $NaBH_4$ reduction.[5] The second step is the synthesis of hitherto unknown 5,6-diphenyldipyrroethane (**4**). Here, the direct conversion of diol to **4** is unsuccessful in the presence of various acid catalysts such as borontrifluoride etherate (BF_3•OEt_2) and trifluoroacetic acid (TFA). Hence, we modified the synthetic route by converting diol into mesylated product using mesyl chloride followed by heating with pyrrole at 40 °C for 2 days to afford **4** in 35% yield.[5] In the final step, the acid-catalyzed oxidative coupling reaction of **4** using *p*-toluenesulfonic acid (*p*-TSA) as the acid catalyst followed by oxidation in presence of 2,3-dichloro-5,6-dicyano-*p*-benzoquinone (DDQ) afforded **6** as a blue fraction in 5% yield. It is pertinent to point out here that all the synthetic methods reported to date involve six to eight steps.[1,2] Hence, the main features of this new synthetic protocol are (1) a reduction in the number of steps from eight to three and (2) simple and straightforward syntheses of precursors and target macrocycles. In support of this, *meso*-tetratolylporphycene (**7**) was synthesized from the respective 5,6-ditolyldipyrroethane (**5**) in 3% yield. Both macrocycles (**6**, **7**) are highly soluble in most of the organic solvents which is not very common in the β-alkyl derivatives[2a,b] and the reported yields are comparable to **3**.[2c] Both **6** and **7** are air-stable and afford violet diamond-shaped crystals from $CHCl_3$/*n*-hexane.

The ^{1}H analysis of **4** and **5** shows signals corresponding to half the linear chain, suggesting the symmetrical nature in which the pyrrole rings are opposite to each other. The structure of **4** is further confirmed by single-crystal X-ray analysis, where the pyrrole rings are trans to each other.[5] The pyrrole and the phenyl rings are arranged in a rectangular fashion to form the two-dimensional supramolecular assembly due to the C−H···$\pi_{pyrrole}$ interaction; the distance and the angles are 2.81 Å and 140.1°, suggesting that the target macrocycle will adopt a rectangular arrangement in the solid state.

The FAB mass spectral analyses of **6** and **7** exhibit a molecular ion signal at *m*/*z* 614 and 670, respectively, indicating the exact composition of the macrocycles. The electronic absorption as well as the emission spectrum of **6** in CH_2Cl_2 is shown in Figure 1, along with the respective

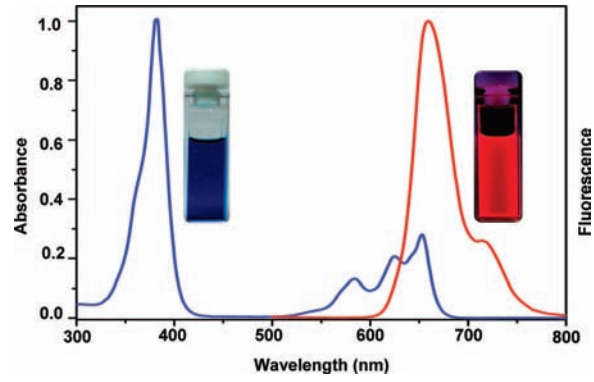

Figure 1. Electronic absorption (blue) and emission (red) spectrum of **6** in CH_2Cl_2. Emission intensity is normalized to the absorption spectrum.

colors. The absorption spectrum of **6** shows the Soret band at 382 nm and Q-bands between 584 to 653 nm. On incorporation of the phenyl rings at the *meso*-positions, a 24 and 9 nm red shift of the Soret band with respect to the parent porphycene[2a] and **3c**[2c] was observed. When compared to **1b**, **6** shows promising features, where the molar extinction coefficient for the Soret band is 3-fold less intense and substantially blue-shifted. In addition, the Q bands appeared at longer wavelength with 1 order of magnitude higher. Furthermore, the emission spectrum of **6** shows a main band at 659 and a weaker band at 715 nm with the quantum yield of Φ_F 0.23 in argon-saturated solutions. Hence, the value is relatively lower than that of **3c** (Φ_F 0.30) and 2-fold higher than **1b** (Φ_F 0.11).

(4) (a) Paolesse, R.; Licoccia, S.; Spagnoli, M.; Boschi, T.; Khoury, R. G.; Smith, K. M. *J. Org. Chem.* **1997**, *62*, 5133–5137. (b) Narayanan, S. J.; Sridevi, B.; Chandrashekar, T. K.; Vij, A.; Roy, R. *Angew. Chem., Int. Ed.* **1998**, *37*, 3394–3397. (c) Sessler, J. L.; Seidel, D.; Lynch, V. *J. Am. Chem. Soc.* **1999**, *121*, 11257–11258. (d) Shimizu, S.; Taniguchi, R.; Osuka, A. *Angew. Chem., Int. Ed.* **2005**, *44*, 2225–2229.

(5) See the Supporting Information.

The ^{1}H spectrum of **6** in CD_2Cl_2 shows aromatic features of porphycene, where the pyrrolic β-CH protons resonate as an AB pattern at 9.39 and 8.32 ppm while the *o*-phenyl protons are observed at 7.65 and the *m*,*p*-phenyl protons resonate at 7.32 ppm as multiplets (Figure 2). Unlike **1b**, the pyrrolic NH proton is shifted to the downfield region and resonates as a broad signal at 5.88 ppm, which suggests that the inner NH protons are in strong intramolecular hydrogen-bonding interaction with the opposite imine nitrogens. This is further confirmed by IR spectral analysis, where broad stretching vibration is observed from 3600 to 3300 cm^{-1}. The presence of NH protons is assigned by CD_2Cl_2/D_2O experiment, where the respective NH signal disappeared. Further, the absence of two α-CH protons in the pyrrolic rings which are observed in **4**, proved by ^{1}H−^{1}H COSY spectral analysis of **6**,[5] where the correlation between the pyrrolic NH proton and the β-CH protons suggests the formation of the macrocycle.

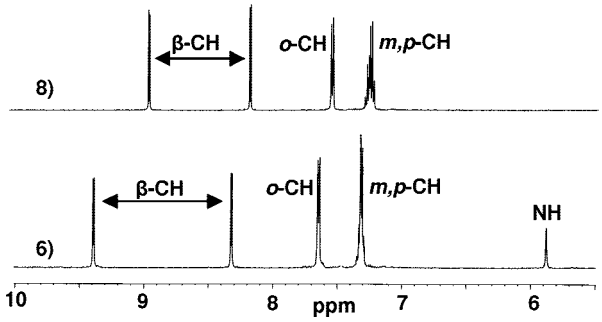

Figure 2. ^{1}H spectra of **6** and **8** in CD_2Cl_2.

The explicit structural detail of the macrocycle **6** is derived from the single-crystal X-ray diffraction analysis (Figure 3a−c),[6] where **6** is a centrosymmetric molecule with C_{2h} symmetry. Consistent with the above observations, α and α′ positions of the pyrroles in one dipyrroethane unit are coupled with another unit to form the macrocycle **6**. The first pyrrole−pyrrole bond is formed from the similar conformation of **4**, and the required planar conformation for the formation of second pyrrole−pyrrole link is achieved through a possible free rotation along C5−C5′ of **4**.[5] The two amino and two imino pyrroles are connected through the *meso*-phenyl-substituted vinylene and/or ethylene bridge, and the amino pyrrolic hydrogen is localized on that particular nitrogen (Figure 3a). It is pertinent to point out here that the amino pyrrolic hydrogens are not localized in any of the porphycene units reported in the literature due to the disorder in the N−H···N hydrogen bonds.[2a−d] There are two strong intramolecular hydrogen bonding interactions with the N−H···N distances and angles of 1.49 Å and 159.6°. As observed in **4**,[5] the macrocycle adopts a rectangular arrangement with N1−N2 and N1−N2′ distances of 2.87 and 2.55 Å, respectively. The distances reported here are similar to **3c** in which the corresponding distances are 2.90 and 2.53 Å.[2c] One of the interesting observations is the presence of intermolecular interactions through C−H···$\pi_{pyrrole}$ with the distance and angle of 2.99 Å and 136° (Figure 3c). It is formed between the hydrogen of the *meso*-phenyl rings with the N1 and N1′ of the pyrrolic π cloud, which generates a one-dimensional supramolecular assembly in the solid state. The *meso*-phenyl rings are almost perpendicular to the mean macrocyclic plane, and the deviations are 79 and 89.6°, respectively. The pyrrole rings are hardly deviated from the mean plane with the maximum deviation of 1.16° with planarity retained (Figure 3b).

The metal coordination chemistry of **6** was investigated using Ni(II) and Pd(II) salts. When **6** was treated with nickel(II) acetylacetonate, in CH_3COOH, blue compound **8** with violet crystals was obtained in quantitative yield. In the presence of palladium(II) acetate, **9** was synthesized in 55% yield (Scheme 1). The metal complexes **8** and **9** were confirmed by FAB mass spectral analysis with its parent ion peak at *m*/*z* 670 and 719, respectively. The electronic absorption spectrum of **8** and **9** showed the Soret band at 393 nm, which was 11 nm red-shifted. The number of Q-bands were reduced to two from three, and the bands were blue-shifted and appeared between 584 and 635 nm as compared to **6**. The slightly upfield shifted pyrrolic β-CH and the *o*- and *m*,*p*-phenyl protons with the disappearance of NH signal from the ^{1}H analysis of **8** (Figure 2) and **9** clearly suggested the insertion of Ni(II) and Pd(II) in **6**.

The final proof of the proposed metal complex (**8**) came from the single-crystal X-ray structure as shown in Figure

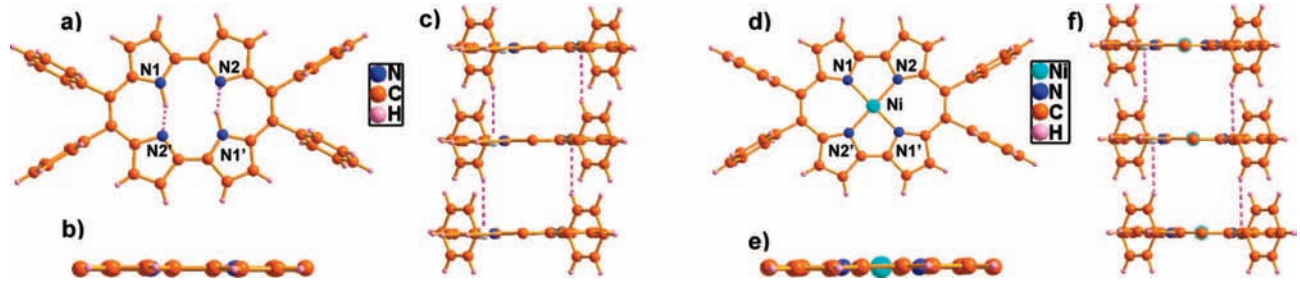

Figure 3. Single-crystal X-ray structures of **6** and **8**. (a, d, b, e): top and side views of **6** and **8**. (c, f): one-dimensional array of **6** and **8**. *meso*-Phenyl groups and the solvent molecules are omitted for clarity in the side view as well as in the 1D array, which is not involved in the H-bonding interaction.

3d−f. As predicted from the spectral analyses, Ni(II) is incorporated inside the macrocyclic ring and the geometry around the metal center is square planar with N1−Ni−N2 and N1−Ni−N2′ angles of 86.8 and 93.2°, respectively (Figure 3d). Conversion of **6** into **8** slightly rearranges the rectangular fashion with N1−N2 and N1−N2′ distances of 2.59 and 2.76 Å, respectively. This leads to a decrease in the N1−N2 distance by 0.28 Å and an increase in the N1−N2′ distance by 0.21 Å. A similar trend was observed in **3c**,[2c] where the respective distances are 2.60(0.30) and 2.74(0.21) Å. Insertion of nickel to the porphycene core retains a one-dimensional array with C−H···$\pi_{pyrrole}$ intermolecular interactions with the distance and angle of 3.02 Å and 135° (Figure 3f). This is generated between the hydrogen of the *meso*-phenyl rings with N2 and N2′ of the pyrrolic π cloud. Further, the maximum deviation of the pyrrole rings is 1.51° and thus maintains the planarity (Figure 3e).

In conclusion, we have demonstrated the syntheses, spectral properties, and one-dimensional supramolecular assembly of 9,10,19,20-tetraarylporphycenes and their metal complexes for the first time. The acid-catalyzed oxidative coupling reaction for porphycene synthesis is an alternative route to the traditional McMurry coupling reaction, used since the discovery of porphycene in 1986.[2a] The aryl groups at the *meso*-position can be properly tuned and find immense application in the area of PDT.[1b] Studies are in progress in this direction in our group.

Acknowledgment. Dr. A.S. thanks DST, New Delhi, and the Director NIIST-CSIR for financial support. A.K.S. thanks CSIR for the fellowship. We thank Dr. Babu Varghese, SAIF, IIT-Chennai, for solving the crystal structure of **4**. We greatly acknowledge Mrs. Viji and Sowmini, NIIST-CSIR, for recording the FAB and NMR spectra.

Supporting Information Available: Synthetic procedures and spectral data for all new compounds. Crystal data for **4**, **6**, and **8** (CIF). This material is available free of charge via the Internet at http://pubs.acs.org.

OL802351R

(6) (a) Crystal data for **6**: $C_{46}H_{32}Cl_6N_4$, M_w = 853.46, triclinic, space group *P*-1, a = 9.2285(14) Å, b = 9.6234(15) Å, c = 11.8311(18) Å, α = 78.780(3)°, β = 76.834(3)°, γ = 73.187(3)°, V = 970.0(3) Å^3, Z = 1, D_{calc} = 1.461 mg/m3, T = 100(2) K, R_1 = 0.0774, wR_2 = 0.1435. (b) Crystal data of **8**: $C_{46}H_{30}Cl_6N_4Ni$, M_w = 910.15, triclinic, space group *P*-1, a = 9.276(2) Å, b = 9.527(3) Å, c = 11.884(3) Å, α = 80.079(5)°, β = 76.283(5)°, γ = 74.095(5)°, V = 974.8(3) Å^3, Z = 1, D_{calc} = 1.550 mg/m3, T = 100(2) K, R_1 = 0.0897, wR_2 = 0.1614. The single-crystal X-ray diffraction data were collected on a Bruker SMART Apex diffractometer equipped with CCD area detector at 100(2) K for **6** and **8**. Good quality single crystals were grown by slow evaporation of *n*-hexane into $CHCl_3$ solutions of **6** and **8**. CCDC-694578 and CCDC-694577 contain the supplementary crystallographic data for **6** and **8**, respectively.